Acta Crystallographica Section B
Structural Science
ISSN 0108-7681

Capabilities and limitations of a (3 + *d*)-dimensional incommensurately modulated structure as a model for the derivation of an extended family of compounds: example of the scheelite-like structures

Alla Arakcheeva* and Gervais Chapuis

École Polytechnique Fédérale de Lausanne, Laboratoire de cristallographie, BSP, CH-1015 Lausanne, Switzerland

Correspondence e-mail: alla.arakcheeva@epfl.ch

Received 17 July 2007
Accepted 14 November 2007

The previously reported incommensurately modulated scheelite-like structure $KNd(MoO_4)_2$ has been exploited as a natural (3 + 1)-dimensional superspace model to generate the scheelite-like three-dimensional structure family. Although each member differs in its space-group symmetry, unit-cell parameters and compositions, in (3 + 1)-dimensional space, they share a common superspace group, a common number of building units in the basic unit cell occupying Wyckoff sites with specific coordinates (x, y, z) and specific basic unit-cell axial ratios (c/a, a/b, b/c) and angles. Variations of the modulation vector **q**, occupation functions and t_0 are exploited for the derivation. Eight topologically and compositionally different known structures are compared with their models derived from the $KNd(MoO_4)_2$ structure in order to evaluate the capabilities and limitations of the incommensurately modulated structure to act as a superspace generating model. Applications of the $KNd(MoO_4)_2$ structure as a starting model for the refinement and prediction of some other modulated members of the family is also illustrated. The (3 + 1)-dimensional presentation of the scheelite-like structures reveals new structural relations, which remain hidden if only conventional three-dimensional structure descriptions are applied.

1. Introduction

For many structural families, the manifold of members is due to different ordered distributions of different atoms or vacancies sharing a common basic structure (Pearson, 1972; Parthé, 1996). This leads to various compositions, various space groups (SGs) and unit cells, which in general cannot be predicted from the common basic structure. In (3 + d)-dimensional superspace, different atomic orderings may be uniquely characterized from a single superspace model (Perez-Mato *et al.*, 1987). The variation of the chemical composition can be quantitatively expressed by periodic occupation functions varying along the internal space dimensions (Perez-Mato *et al.*, 1999); the variation of ordered distributions of the occupations can be expressed in terms of the coefficients α, β and γ defining the modulation wavevector(s) $\mathbf{q}_i = \alpha_i\mathbf{a}^* + \beta_i\mathbf{b}^* + \gamma_i\mathbf{c}^*$ ($\mathbf{a}^*$, $\mathbf{b}^*$ and $\mathbf{c}^*$ are the reciprocal lattice vectors of the basic structure; $i = 1, 2, 3$; each of the α_i, β_i and γ_i coefficients can be rational, irrational or 0; Boullay *et al.*, 2002; Elcoro *et al.*, 2000, 2003, 2004).

The superspace description has already been applied for a few families of compounds. The perovskite-related families of layer structures have been most widely and repeatedly described (for instance: Evain *et al.*, 1998; Gourdon *et al.*, 2000; Boullay *et al.*, 2002; Elcoro *et al.*, 2000, 2003, 2004; Schönleber

© 2008 International Union of Crystallography
Printed in Singapore – all rights reserved

et al., 2004). The $Bi_{2+x}Se_3$ ($x \leq 2$) series (Lind & Lidin, 2003), a group of A_2BX_4 compounds (Chen & Walker, 1990), the MA_xTe_2, where M = Nb, Ta, A = Si, Ge, $\frac{1}{3} < x < \frac{1}{2}$ (van der Lee & Evain, 1995) and $(TS)_nT$ series of hexagonal ferrites (Orlov, Palatinus *et al.*, 2007) are other examples of the unified description of structural families based on a superspace model. The incommensurately modulated structure $Cr_2P_2O_7$ was used as a model for the derivation of the low-temperature lock-in modification (Palatinus *et al.*, 2006). The incommensurately modulated phase of $K_5Yb(MoO_4)_4$ has been exploited to generate the sequence of temperature-dependent phases (Arakcheeva & Chapuis, 2006*a*).

The main objective of the present work is to further develop the application of a single incommensurately modulated structure for crystal chemical considerations. Namely, we exploit the ability of a single incommensurately modulated structure to act as a natural superspace model for the description and prediction of a family of both three-dimensional and (3 + *d*)-dimensional structures differing in chemical composition and topology. This can also be used for the derivation of any possible member of the family. The capabilities and limitations of an incommensurately modulated structure to act as a superspace model is analysed with the example of scheelite-like incommensurately modulated $KNd(MoO_4)_2$ and a series of known three-dimensional structures. The capacity of a single incommensurately modulated structure is directly linked to the properties of (3 + *d*)-dimensional superspace groups (SSGs), which have been introduced for the description of aperiodic crystals (de Wolff *et al.*, 1981), along with additional atomic characteristics associated with the superspace concept (Janssen *et al.*, 2007; van Smaalen, 2004). The ability to reveal some hidden structural relations is illustrated with the scheelite-like structure family presented in the frame of (3 + 1)-dimensional superspace.

2. Why an incommensurately modulated structure can act as a natural superspace model

As repeatedly shown with the examples of perovskite-related compounds (Evain *et al.*, 1998; Gourdon *et al.*, 2000; Boullay *et al.*, 2002; Elcoro *et al.*, 2000, 2003, 2004; Schönleber *et al.*, 2004 among others), the construction of a unique superspace model for a selected family of three-dimensional structures is an elaborate procedure. Even the (3 + *d*)-dimensional SSG selection, which can be performed from the analysis of the reciprocal space, causes certain problems. The main (usually strong) reflections define the common basic structural parameters **a**, **b** and **c**; all other reflections have to be interpreted as satellites with the modulation vector(s) $\mathbf{q}_i = \alpha_i\mathbf{a}^* + \beta_i\mathbf{b}^* + \gamma_i\mathbf{c}^*$, where α_i, β_i and γ_i are specific for each structure. The ambiguity of the choice of the vector(s) $\mathbf{q}_i$ for each individual essentially complicates the SSG selection. Other problems can appear from the ambiguity of the selection of the main reflections, when their intensities are not recognizable as strong ones.

This elaborate procedure can be avoided if a single incommensurately modulated structure belonging to the family is known. Such a structure just exhibits the requested property of the superspace model, *i.e.* the basic structure and the (3 + *d*)-dimensional SSG. The basic structure extracted from an incommensurately modulated structure is characterized by a number of rigid building units in the basic unit cell occupying Wyckoff sites with specific coordinates (x, y, z) and specific unit-cell axial ratios (c/a, a/b, b/c) and cell angles. Each rigid building unit can be an atom as well as a complex ion, a cluster or a molecule. An incommensurately modulated structure also points to the variable parameters, which can be used for the generation of the most probable members. When a certain incommensurately modulated structure is used as a superspace model, a variation of the modulation vector **q**, elemental composition and occupation functions of the Wyckoff sites (and t_0, origin in the x_4 axis, when **q** is rational) can be used for the generation of non-equivalent family members differing in their topology and/or composition (and/or three-dimensional symmetry, when **q** is rational). The variables defined by the symmetry of the Wyckoff sites (variable x, y and z, ADPs and displacive modulations of the building units) characterize each member. These parameters can be obtained from any superspace model with accuracy which ultimately depends on the variation of the chemical composition of the derived family.

Here we would like to underline that not only known structures of a known family can be described using an incommensurately modulated structure, but also an incommensurately modulated structure can be used as the generator of a hypothetical family. Some members of such a hypothetical family could have already been described. In fact, this was the case for the three-dimensional scheelite-like structures described below. Before a search was performed using the ICSD for known scheelite-like structures, we did generate several different three-dimensional structures from the incommensurately modulated $KNd(MoO_4)_2$ reported by Morozov *et al.* (2006).

The capabilities and limitations of an incommensurately modulated structure as a generator of a family in superspace are shown in the next paragraphs with the example of the scheelite-like $KNd(MoO_4)_2$ incommensurately modulated structure (Morozov *et al.*, 2006) and known three-dimensional scheelite-like structures.

3. (3 + 1)-dimensional scheelite-like structure family

3.1. Scheelite-like structures

The scheelite-like family of structures has been widely investigated owing to the luminescent and other optical properties of the corresponding compounds, leading to interesting applications in solid-state lasers (Templeton & Zalkin, 1963; van den Elzen & Rieck, 1973; Jeitschko, 1973; Klevtsova *et al.*, 1975, 1979; Jeitschko *et al.*, 1976; Sleight *et al.*, 1979; Hazen *et al.*, 1985; Huyghe *et al.*, 1991*a*,*b*; Teller, 1992; Shi *et al.*, 1996*a*,*b*, 1997; Stedman *et al.*, 1994; Neeraj *et al.*, 2004;

Table 1
Typical examples of the scheelite-like structures in the (3 + 1)-dimensional presentation in comparison to three-dimensional characterization.

Compound; ICSD code (or reference)	Three-dimensional: Space group; a, b, c (Å) and γ (°) lattice constants; number N of independent atomic sites	(3 + 1)-dimensional: $I2/b(\alpha\beta0)00$ SSG; lattice constants $a \simeq b \simeq 5.5 + 0.5$ Å, $c \simeq 2a$, $\gamma \simeq 90°$; $N = 4$ independent atomic sites	
		Modulation vector $\mathbf{q} = \alpha\mathbf{a}^* + \beta\mathbf{b}^*$ and t_0 for commensurate members	$\Delta_{A,X}$ parameters of the crenel occupation functions
Incommensurate members			
$KNd[MoO_4]_2$† (FIZ supplementary material No. 416200 for Morozov *et al.*, 2006)	None; 5.52, 5.33, 11.90, 90.96; 4	$\mathbf{q} = 0.5779\mathbf{a}^* - 0.1475\mathbf{b}^*$	$\Delta_K = \Delta_{Nd} = \frac{1}{2}$
$KSm[MoO_4]_2$† (Arakcheeva *et al.*, 2007)	None; 5.53, 5.30, 11.78, 91.14; 4	$\mathbf{q} = 0.5677\mathbf{a}^* - 0.1268\mathbf{b}^*$	Wave approximation of occupation function (see text)
$KEu(MoO_4)_2$† (JCPDS PDF2 No. 31-1006)	None; 5.52, 5.28, 11.71, 91.25; 4 (Morozov *et al.*, 2006)	$\mathbf{q} = 0.5641\mathbf{a}^* - 0.1335\mathbf{b}^*$ (predicted in Morozov *et al.*, 2006)	$\Delta_K = \Delta_{Eu} = \frac{1}{2}$
$KLa[MoO_4)_2]$† (PDF-00-040-0466)	None; 5.42, 5.44, 12.21, 90.05; 4 (predicted)	$\mathbf{q} = 0.3507\mathbf{a}^* + 0.6222\mathbf{b}^*$ (predicted)	$\Delta_K = \Delta_{La} = \frac{1}{2}$ (predicted)
Commensurate members			
$RbBi[MoO_4]_2$†; 4181	$P2_1/a$; 5.28, 11.63, 12.09, 92.5; 12	$\mathbf{q} = 0\mathbf{a}^* + \frac{1}{2}\mathbf{b}^*$; $t_0 = 0$	$\Delta_K = \Delta_{Nd} = \frac{1}{2}$
$K_2Th[MoO_4]_3$†; 27734	$A2/a$; 5.36, 17.63, 12.13, 105.8; 10	$\mathbf{q} = 0\mathbf{a}^* + 2/3\mathbf{b}^*$; $t_0 = 0$	$\Delta_K = 2/3$, $\Delta_{Th} = 1/3$
$Eu_2\diamond[WO_4]_3$‡; 15877	$A2/a$; 11.40, 7.68, 11.46, 109.63; 9	$\mathbf{q} = 2/3\mathbf{a}^* + 2/3\mathbf{b}^*$; $t_0 = 0$	$\Delta_{Eu} = 2/3$, $\Delta_\diamond = 1/3$
$Bi_2\diamond MoO_4]_3$‡; 63640	$P2_1/a$; 11.97, 7.71, 11.53, 115.28; 17	$\mathbf{q} = 2/3\mathbf{a}^* + 1/3\mathbf{b}^*$; $t_0 = 0$	$\Delta_{Bi} = 2/3$, $\Delta_\diamond = 1/3$
$La_2\diamond[MoO_4]_3$‡; 2634	$A2/a$; 16.09, 17.01, 11.95, 108.44; 26	$\mathbf{q} = 2/3\mathbf{a}^* + 8/9\mathbf{b}^*$; $t_0 = 0$	$\Delta_{La} = 2/3$, $\Delta_\diamond = 1/3$
$Bi_3[(FeO_4)(MoO_4)_2]$§; 45	$A2/a$; 5.25, 16.90, 11.65, 107.15; 10	$\mathbf{q} = 0\mathbf{a}^* + 2/3\mathbf{b}^*$; $t_0 = 0$	$\Delta_{Mo} = 2/3$, $\Delta_{Fe} = 1/3$
$Na_4Zr[\diamond(MoO_4)_4]$¶; 200914	$I4_1/a$; 11.03, 11.03, 11.68; 7	$\mathbf{q} = 2/5\mathbf{a}^* + 4/5\mathbf{b}^*$; $t_0 = 0$	$\Delta_{Na} = \Delta_{MoO4} = 4/5$, $\Delta_{Zr} = \Delta_\diamond = 1/5$
$Na_4Y[Na'(MoO_4)_4]$††; 78534	$I4_1/a$; 11.37, 11.37, 11.44; 8	$\mathbf{q} = 2/5\mathbf{a}^* + 4/5\mathbf{b}^*$; $t_0 = 0$	$\Delta_{Na} = \Delta_{MoO4} = 4/5$, $\Delta_{Y} = \Delta_{Na'} = 1/5$

† Cations are ordered in A. ‡ Vacancies ($\diamond$) are ordered in A. § Anions are ordered in X. ¶ Both anionic vacancies and cations are ordered in X and A, respectively. †† Partial and ordered replacement of XO_4 tetrahedron by a single cation and ordering of cations in A.

Volkov *et al.*, 2005; Morozov *et al.*, 2006, among many others). The general chemical formula of this family can be expressed as $A[XO_4]$, where A = K, Na, Li, Rb, Ag, Cs, Ca Sr, Ba, Pb, Bi, Zr, Y, Ln and X = Mo, W, V among others. The sheelite-like structures can be generally described as a pair of distorted face-centred cubic (f.c.c.) cells sharing a common face. Both A and XO_4 building units are located at the junctions of each single f.c.c. cell. The lattice periods $a \simeq b$ ($\simeq 5.5 \pm 0.5$ Å) and $c \simeq 2a$, and angles close to 90° are characteristics of the double cell (Fig. 1).

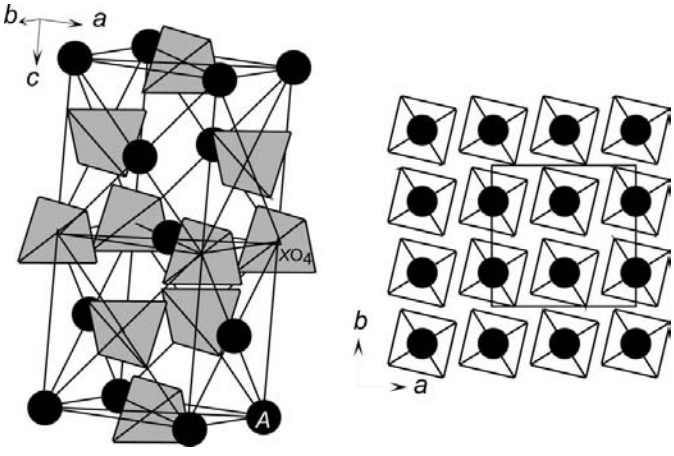

Figure 1
The basic structure and its *ab* projection for the $A[XO_4]$ scheelite-like compounds.

This double cell will be further considered as the basic cell for the description of the family. The A atoms and $[XO_4]$ groups can be either identical or not and also partially vacant, so that the general chemical formula can thus be expressed as $(A', A'')_{n-\delta A}[(X',X'')O_4]_{n-\delta X}$, where $\delta A \geq 0$ and $\delta X \geq 0$ define the vacancies on the corresponding positions. The building units and vacancies can be ordered or randomly distributed on the A and X positions. The ordering affects the symmetry and the unit-cell dimensions in the *ab* plane, whereas the $c \simeq 2a$ translation remains unchanged. As a result, the symmetry of the scheelite-like three-dimensional structures covers a large spectrum from the tetragonal system (space group $I4_1/a$ for the simplest highest-symmetry double f.c.c. cell appearing in scheelite $CaWO_4$; Hazen *et al.*, 1985) to the monoclinic system (various unit cells with monoclinic axis orthogonal to the *ab* plane). Eight known types of ordered distributions of A and $[XO_4]$ building units are presented in Table 1 for different three-dimensional periodic compounds.

The incommensurate (3 + 1)-dimensional structures of $KNd(MoO_4)_2$ (Morozov *et al.*, 2006) and $KSm(MoO_4)_2$ (Arakcheeva *et al.*, 2008) show that an ordered distribution of cations on the A position can also be incommensurate with respect to the **a** and **b** basic structure parameters. Both of them are characterized by their identical SSG and basic structure (Table 1). One of them, namely $KNd(MoO_4)_2$, has been used as a starting model for the refinement of another structure (Arakcheeva *et al.*, 2008), and is here exploited as a superspace model for the derivation of the three-dimensional structures (Table 1) and also for prediction purposes.

Table 2
Three-dimensional space groups derived from the $I2/b(\alpha\beta0)00$ (3 + 1)-dimensional superspace group for $\mathbf{q} = m_1/N_1\mathbf{a}^* + m_2/N_2\mathbf{b}^*$.

In the caption text, m and N are arbitrary integers.

	t_0				
m_1/N_1; m_2/N_2	General	$0 + n/(N_1N_2)$	$1/(4N_1N_2) + n/(N_1N_2)$	$1/(2N_1N_2) + n/(N_1N_2)$	$3/(4N_1N_2) + n/(N_1N_2)$
Odd/even (and 0/1); even/arbitrary	Pa	$P2_1/a$	$P2/a$	$P2_1/a$	$P2/a$
Even/even; even/arbitrary	Pn	$P2_1/n$	$P2/n$	$P2_1/n$	$P2/n$
Even/even; even/even	$I1$	$I\bar{1}$	$I2$	$I\bar{1}$	$I2$
Odd/even (and 0/1); odd/even (and 0/1)	Ib	$I2/b$	$I2/b$	$I2/b$	$I2/b$
Even/general; odd/even (and 0/1)	Pb	$P2_1/b$	$P2/b$	$P2_1/b$	$P2/b$
Even/odd, even/even	Pn	$P2/n$	$P2_1/n$	$P2/n$	$P2_1/n$

3.2. Characteristics of (3 + 1)-dimensional family deduced from the incommensurately modulated $KNd(MoO_4)_2$ structure

3.2.1. Main characteristics. The $KNd(MoO_4)_2$ structure exhibits the following (3 + 1)-dimensional superspace model characteristics, which can be attributed to the $(A',A'')_{n-\delta A}[(X',X'')O_4]_{n-\delta X}$ sheelite-like family.

(i) Monoclinic SSG is $I2/b(\alpha\beta0)00$, with modulation vector $\mathbf{q} = \alpha\mathbf{a}^* + \beta\mathbf{b}^*$, where α and β are variables.

(ii) The basic unit cell is characterized by $a/b \simeq 1$, $c/a \simeq c/b \simeq 2$, $a \simeq 5.5$ Å, $\gamma \simeq 90^\circ$.

(iii) The basic structure consists of four atomic positions: A [4(*e*): $\frac{1}{2}\frac{1}{4}\,z_A \simeq 0.88$], X [4(*e*): $\frac{1}{2}\frac{1}{4}\,z_X \simeq z_A - 0.5$], O1 [8(*f*): $x \simeq 0.36$, $y \simeq 0.02$, $z \simeq 0.29$], O2 [8(*f*): $x \simeq 0.77$, $y \simeq 0.41$, $z \simeq 0.04$]. Two building unit positions corresponding to the A and X sites should preferably be used for the basic structure description.

(iv) The occupation function of the A position, $o[A]$, defines the ordered distribution of A' and A'' on A (Morozov *et al.*, 2006); hence, this function can vary with composition and ordering. The symmetry of the A and X sites is identical; hence, the occupation function of the $[XO_4]$ building unit can also vary.

(v) The ordering of the building units on the A site (consequently on X) is the origin of the structure modulations that can be described by different occupation modulation functions; the displacive modulations of the atoms are a consequence of the occupation modulations and they play the role of maintaining reasonable cation–oxygen distances (Morozov *et al.*, 2006).

Different commensurate and incommensurate structures can be generated by varying the α and β components of the modulation vector $\mathbf{q}$, and the site occupation functions of both A and X. For the commensurate cases with rational α and β, the initial phase of the modulation selected along the x_4 axis (t_0 value) is also variable for each combination of α and β; the choice of t_0 selects the SG derived from the SSG (see, for example, Perez-Mato *et al.*, 1999).

3.2.2. Possible occupation functions. It is evident from the characteristics presented above that the primary variable in the family depends on the A and X site occupations.

Similar to $KNd(MoO_4)_2$, the occupation function of A (X) can be defined by crenel functions as $o[A'(X')] = 1$ and $o[A''(X'')] = 1$ in the $\Delta_{A'(X')}$ and respectively $\Delta_{A''(X'')}$ domain range of t, where $A'(X')$ and $A''(X'')$ express different building units or vacancies. According to the SSG and symmetry of the A (X) position, the centre of the $\Delta A'X'$ and $\Delta A''(X'')$ ranges corresponds to $x_4^0 = 0$ and $x_4^0 = 0.5$ along x_4. The ratios $\Delta_{A'}/\Delta_{A''}$ and $\Delta_{X'}/\Delta_{X''}$ define the ratios A'/A'' and X'/X'' in the

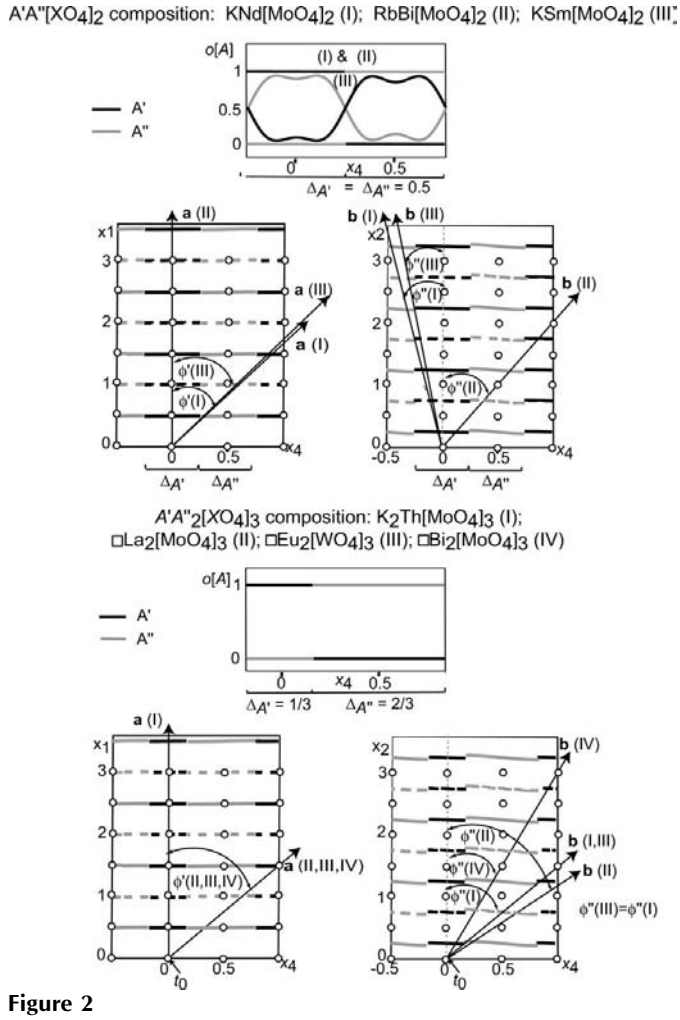

Figure 2
Illustrations of the derivation of the scheelite-like structures from the incommensurately modulated $KNd[MoO_4]_2$ [SSG $I2/b(\alpha\beta0)00$]. Occupation functions, $o[A]$, are indicated along the internal x_4 axis for two groups of compounds specified by numbers in brackets. For every compound, the **a** and **b** axes are shown in geometrically transformed sections of the (3 + 1)-dimensional direct space: x_1x_4 [$x_2 = 1/4$, $x_3 = 0.88$ (dashed line) and $x_3 = 0.38$ (solid line)] and x_2x_4 [$x_1 = 0$, $x_3 = 0.88$ (dashed line) and 0.38 (solid line)]; $\mathrm{tg}(\varphi') = \alpha$ and $\mathrm{tg}(\varphi'') = \beta$ in the $\mathbf{q} = \alpha\mathbf{a}^* + \beta\mathbf{b}^*$. Empty circles indicate centres of inversion.

Table 3
Fractional coordinates of A = Rb, Bi and X = Mo generated from the incommensurately modulated $KNd[MoO_4]_2$ for $RbBi[MoO_4]_2$ compared with the experimental data reported by Klevtsova *et al.* (1975) (SG $P2_1/a$; a = 5.28, b = 11.63, c = 12.09 Å, γ = 92.5°).

	X		Y		Z	
Position	Generated	Experimental	Generated	Experimental	Generated	Experimental
Bi 4(*e*)	0.5013	0.5054 (5)	0.1155	0.1211 (2)	0.8755	0.8769 (2)
Rb 4(*e*)	0.4956	0.5167 (8)	0.3780	0.3781 (3)	0.1237	0.1244 (3)
Mo1 4(*e*)	0.5204	0.5213 (9)	0.1276	0.1143 (3)	0.3697	0.3874 (3)
Mo2 4(*e*)	0.5204	0.4998 (9)	0.3767	0.3444 (3)	0.6149	0.6456 (3)

Table 4
Fractional coordinates of A = K, Th and X = Mo generated from the incommensurately modulated $KNd[MoO_4]_2$ for $K_2Th[MoO_4]_3$ compared with the experimental data reported by (upper line) Huyghe *et al.* (1991*a*) (SG $A2/a$; a = 5.3688, b = 17.6649, c = 12.143 Å, γ = 108.756°) and (lower line) by Bushuev & Trunov (1976) (SG $A2/a$; a = 5.363, b = 17.62999, c = 12.13 Å, γ = 108.8°).

	X		Y		Z	
Position	Generated	Experimental	Generated	Experimental	Generated	Experimental
Th 4(*e*)	0.75	0.75	0.5	0.5	0.3763	0.373758 (8)
		0.75		0.5		0.3631 (2)
K 8(*f*)	0.4242	0.4228 (1)	0.1691	0.16630 (4)	0.3699	0.37765 (5)
		0.4278 (12)		0.1705 (2)		0.368 (8)
Mo1 4(*e*)	0.25	0.25	0.5	0.5	0.1165	0.14508 (2)
		0.25		0.5		0.1233 (1)
Mo2 8(*f*)	0.1070	0.10186 (4)	0.0.3320	0.34353 (1)	0.3671	0.38910 (2)
		0.1014 (1)		0.3445 (1)		0.3745 (1)

Table 5
Fractional coordinates of A = Bi, X' = Fe and X'' = Mo generated from the incommensurately modulated $KNd[MoO_4]_2$ for $Bi_3[(FeO_4)(MoO_4)_2]$ compared with the experimental data reported by Jeitschko *et al.* (1976) (SG $A2/a$; a = 5.254, b = 16.90399, c = 11.653 Å, γ = 107.15°).

	X		Y		Z	
Position	Generated	Experimental	Generated	Experimental	Generated	Experimental
Bi2 4(*e*)	0.25	0.25	0	0	0.6237	0.65514 (11)
Bi1 8(*f*)	0.4073	0.4058 (2)	0.1589	0.15163 (6)	0.8672	0.88679 (9)
Fe1 4(*e*)	0.25	0.25	0	0	0.1165	0.1178 (5)
Mo1 8(*f*)	0.3930	0.4234 (4)	0.1681	0.16811 (12)	0.3671	0.3722 (2)

chemical composition of the expected compound. Two kinds of crenel occupation functions are used in Fig. 2 for the compounds considered in this work (Table 1). The first one ($\Delta_{A'}/\Delta_{A''} = 1$; $\Delta_{A'} = \Delta_{A''} = 0.5$) corresponds to the general composition $A'A''[X'O_4]_2$, the second one ($\Delta_{A'}/\Delta_{A''} = 2$; $\Delta_{A'} = 2/3$, $\Delta_{A''} = 1/3$) corresponds to $A'A''_2[X'O_4]_3$. The crenel function with $\Delta_{X''}/\Delta_{X'} = 2$ ($\Delta_{X'} = 2/3$, $\Delta_{X''} = 1/3$) has been applied for the general composition $A_3[X'O_4]_2[X''O_4]$.

Typical crenel functions used in a superspace model generate a completely ordered distribution of building units on the A (X) position, *i.e.* either A' (X') or A'' (X'') can be found at any position. Partially ordered distributions of A' (X') and A'' (X'') on the A (X) position can be approximated by occupation functions consisting of a few harmonic terms, when two complementary waves are attributed to A' (X') and A'' (X'') building units, respectively. This type of occupation function has been applied to the refinement of the scheelite-like incommensurately modulated structure $KSm[MoO_4]_2$ (Table 1; Arakcheeva *et al.*, 2008). An example of the wave occupation function is shown in Fig. 2 along with two crenel functions. Other kinds of occupation function are also possible in the family.

3.2.3. Possible space groups derived from *I*2/*b*(*αβ*0)00. The main algorithms of derivations of SGs from a SSG for rational coefficient(s) of the modulation vector(s) **q** can be found in Yamamoto & Nakazawa (1982), Perez-Mato *et al.* (1987) and Janssen *et al.* (2007). A database currently available at http://superspace.epfl.ch/finder/ (Orlov, Schoeni *et al.*, 2007) provides a convenient environment to extract the required information. The *JANA*2000 program package (Petříček *et al.*, 2000) has been used in the present study for the derivation of SGs from the SSG $I2/b(\alpha\beta0)00$.

The symmetry operations of $I2/b(\alpha\beta0)00$ are:

(i) $(E1 \mid n_1\ n_2\ n_3\ n_4)$;
(ii) $(2_z - 1 \mid 0\ \frac{1}{2}\ 0\ 0)$;
(iii) $(b_z\ 1 \mid 0\ \frac{1}{2}\ 0\ 0)$;
(iv) $(i\ -1 \mid 0\ 0\ 0\ 0)$; + $(E\ 1 \mid \frac{1}{2}\ \frac{1}{2}\ \frac{1}{2}\ 0)$.

If the α and β coefficients of the vector **q** are rational, *i.e.* $\mathbf{q} = m1/N_1\mathbf{a}^* + m_2/N_2\mathbf{b}^*$, the SGs listed in Table 2 can be derived from this SSG for the supercell with parameters $a_S = N_1 a_{basic}$ and $b_S = N_2 b_{basic}$. Special cases of $\alpha = m_1/N_1$ and $\beta = m_2/N_2$ result in additional centring of the supercell. If $N1$ and $N2$ have no common divisor other than 1, then there is no additional centring. Otherwise the following reflection condition occurs: $h + nk = dP_1$, where n must be selected so that $m_1 + nm_2 = dP_2$, where P_1 and P_2 are arbitrary integers and d is the greatest common divisor of N_1 and N_2.

3.3. Derivation of three-dimensional scheelite-like structures from the incommensurately modulated $KNd(MoO_4)_2$

In order to evaluate the capabilities and limitations of the incommensurately modulated structure $KNd(MoO_4)_2$ as a superspace model, eight known three-dimensional scheelite-like compounds (Table 1) have been generated from the model. All are characterized by different compositions and different distributions of atoms on the A and X positions. By generation, we understand the derivation of the unit cell, the SG and atomic coordinates from the structural characteristics of $KNd(MoO_4)_2$ (FIZ supplementary materials No. 416200 for Morozov *et al.*, 2006) by exploring the modulation vector **q**, and the occupation functions of both A and X, and t_0. The *JANA*2000 program package (Petříček *et al.*, 2000) has been

used for all calculations. The results are presented in Table 3–11 and illustrated in Figs. 2–7 and compared with experimental data. The experimental SGs and unit-cell parameters presented in Table 1 are expressed in the monoclinic setting with angle γ.

For each structure, the modulation vector $\mathbf{q} = m_1/N_1\mathbf{a}^* + m_2/N_2\mathbf{b}^*$ has been determined from the reciprocal space analysis, taking into account the reflection condition [$hk0m$: $h + k = 2n$] characteristic of the SSG $I2/b(\alpha\beta0)00$. The $hk0$ reciprocal space sections have been reconstructed using the structural data included in the ICSD database and reported in the original papers. The values of Δ_A and Δ_X defining the corresponding crenel occupation functions have been selected according to the chemical composition of each compound. For each monoclinic structure, the supercell with parameter $a_S = N_1 a_{basic}$ and $b_S = N_2 b_{basic}$ has been derived from the superspace model. In the cases when N_1 and N_2 have no common divisor except 1, the SG has been derived from the SSG $I2/b(\alpha\beta0)00$ for the supercell by selecting a value of t_0 (Table 2, Fig. 2) in accordance with the experimental SG. When N_1 and N_2 have a common divisor distinct from 1, the unit cell and corresponding SG have been selected according to the additional centring (see §3.2.3), and also with respect to the unit cell selected in the experimental study (Fig. 5). For the tetragonal structures, the monoclinic $I2/b$ SG derived from the SSG $I2/b(\alpha\beta0)00$ has been selected as a subgroup of the

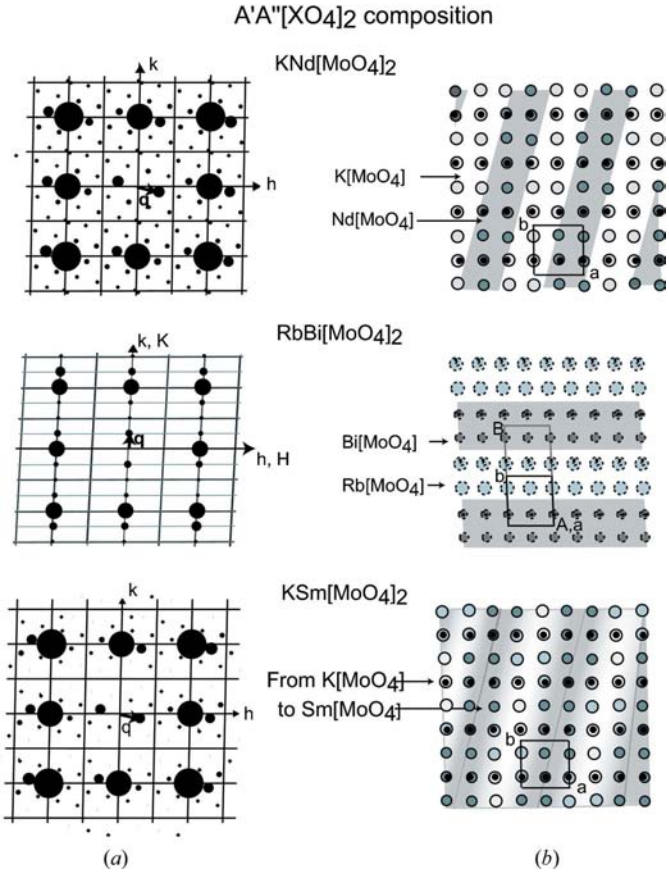

Figure 3
$hk0$ sections of reciprocal space (*a*) and *ab* projections (*b*) for the monoclinic scheelite-like compounds with the composition $A'A''[XO_4]_2$. Solid lines and small letters refer to the basic structure characteristics described in (3 + 1)-dimensional space; the grey lines and capital letters refer to three-dimensional descriptions. The strongest reflections, $hk00$, justify the selection of the basic structure parameters **a** and **b**. In the *ab* projections, O atoms are omitted; small black circles indicate *X* atoms; dashed contours refer to simulated atomic positions; grey and white areas refer to the given composition. The compositional wave direction coincides with the modulation vector **q**. $KNd[MoO_4]_2$ and $KSm[MoO_4]_2$ refer to refined incommensurately modulated structures reported in Morozov *et al.* (2006) and Arakcheeva *et al.* (2008), respectively.

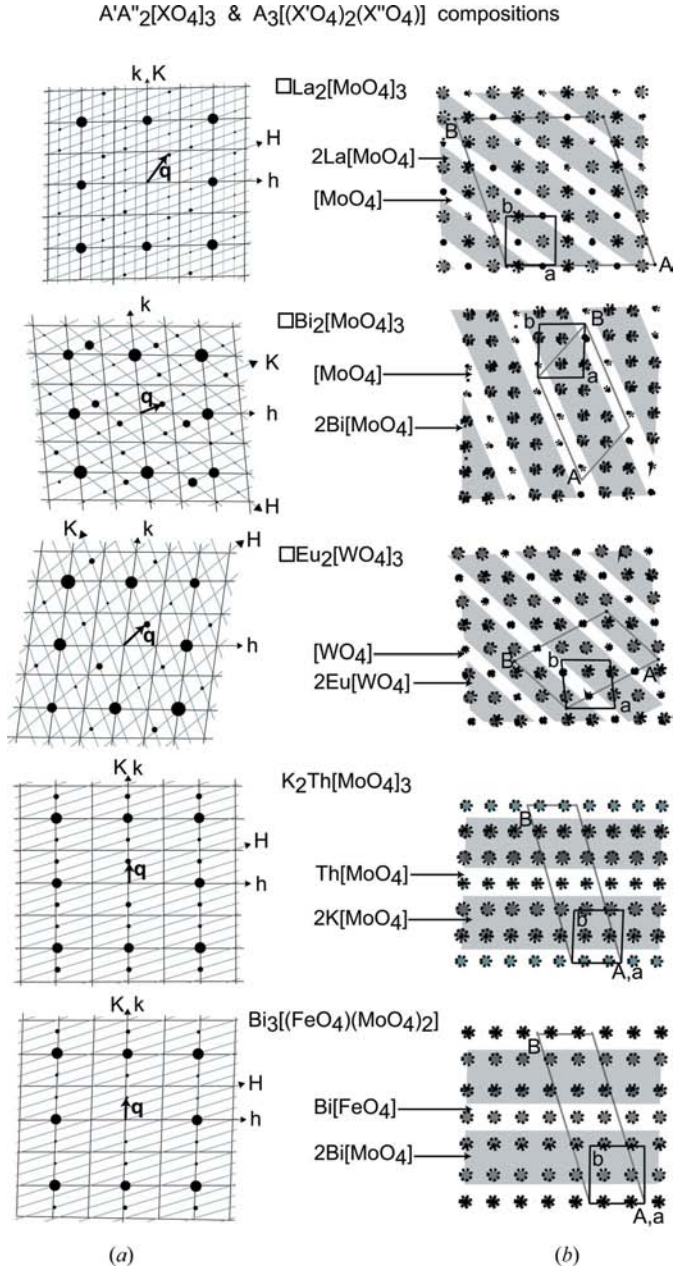

Figure 4
$hk0$ sections of reciprocal space (*a*) and *ab* projections (*b*) for the monoclinic scheelite-like compounds with the compositions $A'A''_2[XO_4]_3$ and $A_3[(X'O_4)(X''O_4)_2]$. All notations are similar to Fig. 2. In $La_2[MoO_4]_3$, $Bi_2[MoO_4]_3$ and $Eu_2[MoO_4]_3$, A' is assumed to be a vacancy indicated by square in the chemical formulae.

Table 6
Fractional coordinates of A'' = Eu and X = WO_4 generated from the incommensurately modulated structure $KNd[MoO_4]_2$ for $Eu_2[WO_4]_3$ compared with the experimental data reported by Templeton & Zalkin (1963) (SG $A2/a$; a = 11.396, b = 7.676, c = 11.463 Å, γ = 115.40°).

	X		Y		Z	
Position	Generated	Experimental	Generated	Experimental	Generated	Experimental
Eu 8(*f*)	0.4166	0.4066 (2)	0.3333	0.3338 (2)	0.3773	0.3768 (1)
W1 4(*e*)	0.25	0.25	0	0	0.1335	0.1318 (2)
W2 4(*e*)	0.0903	0.0507 (1)	0.1555	0.1452 (2)	0.3829	0.3935 (1)

Table 7
Fractional coordinates of A'' = Bi and X = MoO_4 generated from the incommensurately modulated $KNd[MoO_4]_2$ for $Bi_2[MoO_4]_3$ compared with the experimental data reported (upper line) by Theobald & Laarif (1985) (SG $P2_1/a$; a = 11.972, b = 7.7104, c = 11.5313 Å, γ = 115.276°) and (lower line) by van den Elzen & Rieck (1973) (SG $P2_1/a$; a = 11.929, b = 7.685, c = 11.491 Å, γ = 115.40°).

	X		Y		Z	
Position	Generated	Experimental	Generated	Experimental	Generated	Experimental
Bi1 4(*f*)	0.2583	0.2607 (4)	0.2398	0.2552 (7)	0.3797	0.3612 (4)
		0.25584 (5)		0.25999 (8)		0.36188 (5)
Bi2 4(*e*)	0.0792	0.0840 (5)	0.9218	0.9055 (8)	0.1255	0.1314 (4)
		0.08334 (6)		0.90798 (10)		0.12976 (5)
Mo1 4(*e*)	0.4111	0.4150 (5)	0.0745	0.0254 (9)	0.1320	0.1122 (5)
		0.4165 (1)		0.0320 (2)		0.1114 (1)
Mo2 4(*e*)	0.0778	0.1037 (5)	0.4078	0.4288 (10)	0.1121	0.1496 (5)
		0.1089 (1)		0.4218 (2)		0.1513 (1)
Mo3 4(*e*)	0.2612	0.1943 (5)	0.7677	0.7325 (9)	0.3774	0.3685 (6)
		0.1952 (1)		0.7341 (2)		0.3669 (1)

Table 8
Fractional coordinates of A'' = La and X = Mo generated from the incommensurately modulated $KNd[MoO_4]_2$ for $La_2[MoO_4]_3$ compared with the experimental data reported by Jeitschko (1973) (SG $A2/a$; a = 16.093, b = 17.006, c = 11.952 Å, γ = 108.44°).

	X		Y		Z	
Position	Generated	Experimental	Generated	Experimental	Generated	Experimental
La1 8(*f*)	0.0802	0.08908 (6)	−0.0077	0.00680 (5)	0.6267	0.62464 (8)
La2 8(*f*)	0.3068	0.30250 (6)	0.1697	0.16545 (6)	0.1241	0.12766 (7)
La3 8(*f*)	0.4687	0.47751 (6)	0.1579	0.16552 (6)	0.8692	0.87816 (7)
Mo1 8(*f*)	0.4245	0.42092 (9)	−0.0014	0.00723 (8)	0.1220	0.12871 (13)
Mo2 8(*f*)	0.3087	0.30928 (10)	0.1661	0.166659 (10)	0.6172	0.63204 (12)
Mo3 8(*f*)	0.1447	0.13722 (10)	0.1656	0.17144 (9)	0.3642	0.37590 (11)
Mo4 8(*f*)	0.4633	0.46572 (10)	0.1682	0.16166 (10)	0.3707	0.38554 (11)
Mo5 4(*e*)	0.25	0.25	0	0	0.8617	0.87311 (16)

experimental SG $I4_1/a$. The experimental lattice parameters have been used for the illustrations (Figs. 3–7) of each derived structure.

3.3.1. Structures with ordering of cations on *A* position. Similar to the incommensurately modulated structures of $KNd[MoO_4]_2$ and $KSm[MoO_4]_2$, the three-dimensional structure of $RbBi[MoO_4]_2$ (Klevtsova *et al.*, 1975) belongs to the group with the general composition $A'A''[X'O_4]_2$ and exhibits a cation ordering on the A position (Table 1, Fig. 3). The crenel occupation function $\Delta_{Rb} = \Delta_{Bi}$ (Fig. 2) corresponding to this composition, and the modulation vector $\mathbf{q} = 0\mathbf{a}^* + \frac{1}{2}\mathbf{b}^*$ (Fig. 3) have been used to generate the $RbBi[MoO_4]_2$ structure. For $\mathbf{q} = 0\mathbf{a}^* + \frac{1}{2}\mathbf{b}^*$, the SGs $P2_1/a$ ($t_0 = 0 + n/4$), $P2/a$ ($t_0 = 1/8 + n/4$) and Pa (for other values of t_0) are possible for the supercell with parameters $a_S = a_{basic}$, $b_S = 2b_{basic}$ (Table 2, Fig. 5). The origin $t_0 = 0$ has been selected according to the experimental SG $P2_1/a$ (Table 1). The generated structure was transformed by the matrix $(100; 0\bar{1}0; 00\bar{1})$ in order to match the atomic positions reported by Klevtsova *et al.* (1975). The generated coordinates of Rb, Bi and Mo are given in Table 3 along with the experimental data; a comparison of the *ab* structure projections is shown in Fig. 6.

$K_2Th[MoO_4]_3$ (Bushuev & Trunov, 1976; Huyghe *et al.*, 1991*a*) gives another example of a cation ordering on the A position. This example differs by the general composition $A'A''_2[X'O_4]_3$ resulting in a crenel occupation function with $\Delta_K/\Delta_{Th} = 2$ (Fig. 2). For $\mathbf{q} = 0\mathbf{a}^* + 2/3\mathbf{b}^*$ (Fig. 4), the SGs $I2/b$ ($t0 = 0 + n/6$) and Ib (for other values of t_0) are possible for the supercell with parameters $a_S = a_{basic}$, $b_S = 3b_{basic}$ (Table 2, Fig. 5). The origin $t_0 = 0$ has been selected. The generated model has been transformed by the matrix $(\bar{1}00/1\bar{1}0/001)$ (Fig. 5) and shifted by 0.5*a* and 0.5*c* in order to compare with SG $A2/a$ and atomic positions reported by Huyghe *et al.* (1991*a*). Two sets of K, Th and Mo coordinates are listed in Table 4; the corresponding *ab* projections are shown in Fig. 6. The structures of $Na_2Zr(MoO_4)_3$ (Klevtsova *et al.*, 1979), $Bi_3Zr(MoO_4)_3$ among others correspond to the same structure type.

3.3.2. Structures with ordering of [XO_4] on the *X* position. The structure of $Bi_3[(FeO_4)(MoO_4)_2]$ (Jeitschko *et al.*, 1976) is an example of anionic building unit ordering on the X position. According to the general composition $A_3[(X'O_4)(X''O_4)_2]$, the crenel occupation function with $\Delta_{Mo}/\Delta_{Fe} = 2$ has been applied to the X position. Since both the $\mathbf{q} = 0\mathbf{a}^* + 2/3\mathbf{b}^*$ and the experimental SGs are identical for $Bi_3[(FeO_4)(MoO_4)_2]$ and $K_2Th[MoO_4]_3$ (Table 1, Fig. 4), identical supercells have been selected for the derivation of these two structures (Fig. 5). The set of atomic coordinates derived for $Bi_3[(FeO_4)(MoO_4)_2]$ was shifted by 0.5*a* for comparison with the published data (Table 5, Fig. 6). The structures of $Bi_3[(Sc,Bi)O_4(MoO_4)_2]$ (Kolitsch & Tillmanns, 2003) and $Bi_3[(GaO_4)(MoO_4)_2]$ (Jeitschko *et al.*, 1976) among others correspond to the same structure type.

3.3.3. Structures with vacancy ordering on the *A* positions. $La_2[MoO_4]_3$ (Jeitschko, 1973), $Eu_2[WO_4]_3$ (Templeton & Zalkin, 1963) and $Bi_2[MoO_4]_3$ (Theobald & Laarif, 1985) with the general composition $A'A''_2[X'O_4]_3$, where A' indicates a vacancy, are considered in the original publications as schee-

lite-like structures with different vacancy distributions on the *A* position resulting in different SGs and different *a* and *b* unit-cell parameters (Table 1). By exploring the incommensurately modulated structure $KNd[MoO_4]_2$ in superspace, the vacancy distributions are generated with identical crenel functions ($\Delta_{A''}/\Delta_{A'} = 2$ in Fig. 2) defined by the common general composition, while the modulation vectors **q** (Fig. 4) identify each individual.

For $Eu_2[WO_4]_3$, **q** = 2/3**a*** + 2/3**b*** (Fig. 4) was selected. For this special value, the possible SGs are $X2/b$ ($t_0 = 0 + n/3$) and Xb (for other values of t_0), where X refers to the non-primitive [000; 5/6 1/6 1/2; 2/3 1/3 0; 1/3 2/3 0; 1/2 1/2 1/2; 1/6 5/6 1/2] centring of the supercell with parameters $a_S = 3a_{basic}$ and $b_S = 3b_{basic}$ (Fig. 5). The origin $t_0 = 0$ has been selected according to the experimental centrosymmetric SG of the structure (Table 1). The generated model transformed (Fig. 5) by the matrix (−2/3 −1/3 0; 1/3 −1/3 0; 001) and shifted by 0.5*c* can be compared with the atomic positions reported by Templeton & Zalkin (1963). The Eu and W coordinates and the *ab* superstructure projections are compared in Table 6 and Fig. 6, respectively.

For $Bi_2[MoO_4]_3$, **q** = 2/3**a*** + 1/3**b*** (Fig. 4) allows the SGs $X2_1/a$ ($t_0 = 0 + n/3$), $X2/a$ ($t_0 = 1/12 + n/3$) and Xa (for other values of t_0), where X refers to the non-primitive [000; 1/3 1/3 0; 2/3 2/3 0] centring of the supercell with parameters $a_S = 3a_{basic}$ and $b_S = 3b_{basic}$ (Fig. 5). The origin $t_0 = 0$ has been selected according to the experimental centrosymmetric SG (Table 1). The generated model transformed (Fig. 5) by the matrix (−1/3 2/3 0; −1/3 −1/3 0; 001) and shifted by 0.5*b* can be compared with the atomic positions reported by Theobald & Laarif (1985) and van den Elzen & Rieck (1973). The

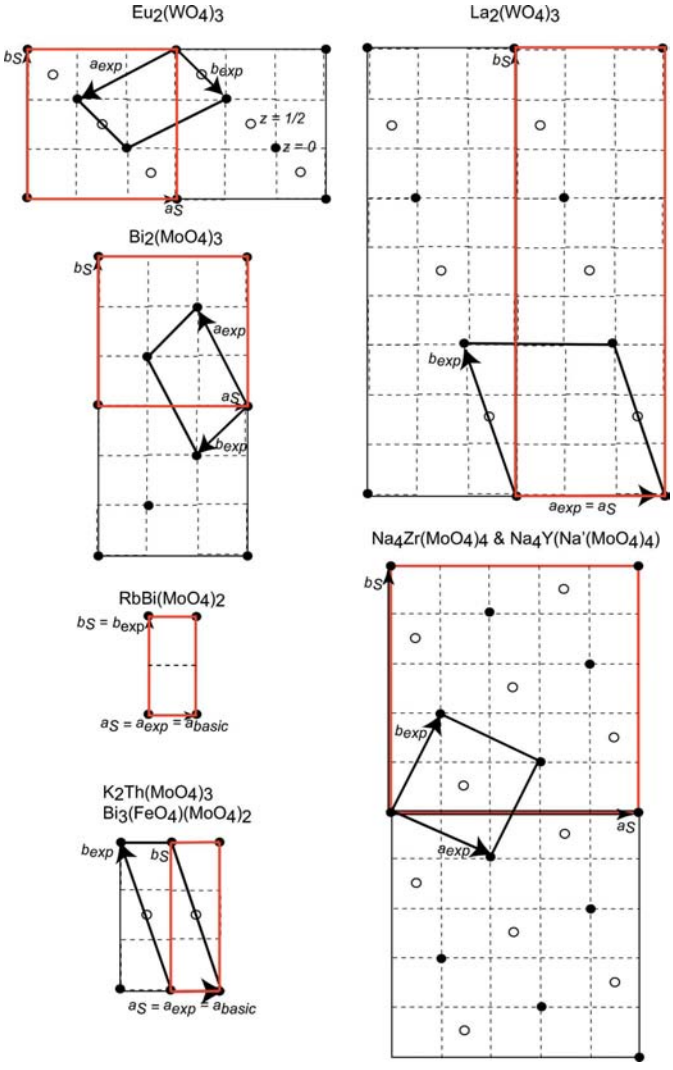

Figure 5
Selection of the experimental unit cell from the supercell (red box) generated for the commensurately modulated scheelite-like structures. The a_Sb_S supercell is centred (black circle for $z = 0$, open circle for $z = \frac{1}{2}$) for each compound except $RbBi(MoO_4)_2$. Dashed lines indicate the basic unit cell.

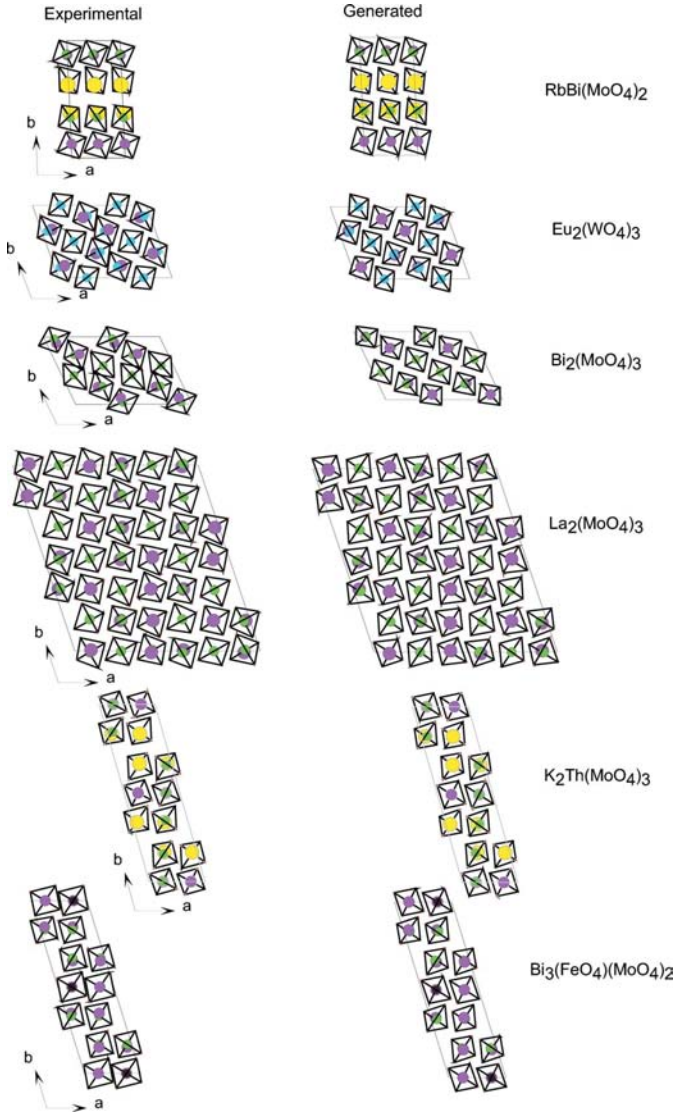

Figure 6
Experimental and generated *ab* projections of some scheelite-like structures with different topologies. The experimental unit cells are indicated. The $[XO_4]$ groups are shown as tetrahedra centred by green, blue and brown spheres corresponding to X = Mo, W and Fe atoms, respectively. The yellow spheres indicate K and Rb. The pink spheres refer to Eu, Bi, La and Th.

Table 9
Fractional coordinates of A' = Na, A'' = Zr and X' = Mo generated from the incommensurately modulated $KNd[MoO_4]_2$ for $Na_4Zr[MoO_4]_4$ compared with the experimental data reported by Klevtsova *et al.* (1979).

Atomic coordinates are adapted to SG $I2/b$ ($\gamma = 90°$; origin in the centre of inversion) derived from experimental SG $I4_1/a$ ($a = b = 11.03$, $c = 11.952$ Å).

	X		*Y*		*Z*	
Position	Generated	Experimental	Generated	Experimental	Generated	Experimental
Mo1 8(*f*)	0.2119	0.1794	0.3537	0.3356	0.3692	0.3720
Mo2 8(*f*)	0.5927	0.5856	0.0477	0.0706	0.6186	0.6220
Zr 4(*e*)	0	0	0.25	0.25	0.1350	0.125
Na1 8(*f*)	0.1992	0.2270	0.3456	0.3670	−0.1336	−0.0910
Na2 8(*f*)	0.6005	0.6170	0.0527	0.0230	0.1540	0.1590

Table 10
Fractional coordinates of the A' = Na, A'' = Y, X' = Mo and X'' = Na′ generated from the incommensurately modulated $KNd[MoO_4]_2$ for $Na_4Y[Na'(MoO_4)_4]$ compared with the experimental data reported by Stedman *et al.* (1994).

Atomic coordinates are adapted to SG $I2/b$ ($\gamma = 90°$; origin in the centre of inversion) derived from experimental SG $I4_1/a$ ($a = b = 11.37$, $c = 11.44$ Å).

	X		*Y*		*Z*	
Position	Generated	Experimental	Generated	Experimental	Generated	Experimental
Mo1 8(*f*)	0.2119	0.1811 (3)	0.3537	0.34359 (2)	0.3692	0.38685 (2)
Mo2 8(*f*)	0.5927	0.59359 (2)	0.0477	0.0689 (3)	0.6186	0.63685 (2)
Y 4(*e*)	0	0	0.25	0.25	0.1350	0.125
Na1 8(*f*)	0.1992	0.2044 (2)	0.3456	0.3704 (2)	−0.1336	−0.0840 (2)
Na2 8(*f*)	0.6005	0.6204 (2)	0.0527	0.0456 (2)	0.1540	0.1560 (2)
Na′ 4(*e*)	0	0	0.25	0.25	0.6376	0.625

comparison of Bi and Mo coordinates is presented in Table 7; comparison of the *ab* superstructure projections is shown in Fig. 6.

For $La_2[MoO_4]_3$, the modulation vector $\mathbf{q} = 2/3\mathbf{a}^* + 8/9\mathbf{b}^*$ (Fig. 4) generates SGs $X2/b$ ($t_0 = 0 + n/9$) and Xb (for other values of t_0), where X refers to the non-primitive centring [000; 5/6 1/6 1/2; 2/3 1/3 0; 1/3 2/3 0; 1/2 1/2 1/2; 1/6 5/6 1/2] of the supercell with parameters $a_S = 3a_{basic}$ and $b_S = 9b_{basic}$ (Fig. 5). The origin $t_0 = 0$ has been selected according to the experimental centrosymmetric SG (Table 1). The generated model transformed (Fig. 5) by the matrix (1 0 0; −1/3 1/3 0; 001) and shifted by $0.5c$ can be compared with the atomic positions reported by Jeitschko (1973). The comparison of La and Mo coordinates is presented in Table 8, whereas the *ab* superstructure projections are compared in Fig. 6.

3.3.4. Structures with cation ordering on *A* and vacancy ordering on *X* positions. The tetragonal structure of $Na_4Zr[MoO_4]_4$ (Klevtsova *et al.*, 1979; Table 1) with the general composition $A'_4A''[\diamond(X''O_4)_4]$, where $\diamond$ denotes the $[X'O_4]$ tetrahedron which is missing on every fifth X position, has been generated in the monoclinic $I2/b$ SG, which is a subgroup of the experimental tetragonal $I4_1/a$ SG. According to the composition, the crenel functions with $\Delta_{Na}/\Delta_{Zr} = 4$ and $\Delta_{[MoO_4]}/\Delta_{\diamond} = 4$ (Fig. 7) reproduce the structure when applied respectively on A and $X(O_4)$. The selected vector $\mathbf{q} = 2/5\mathbf{a}^* + 4/5\mathbf{b}^*$ (Fig. 7) generates SGs $X2/b$ ($t_0 = 0 + n/5$) and Xb (for other values of t_0), where X refers to the non-primitive centring [3/10 1/10 1/2; 3/5 1/5 0; 1/5 2/5 0; 4/5 3/5 0; 2/5 4/5 0; 9/10 3/10 1/2; 1/2 1/2 1/2; 1/10 7/10 1/2; 7/10 9/10 1/2] of the superstructure unit cell with parameters $a_S = 5a_{basic}$ and $b_S = 5b_{basic}$ (Fig. 5). The generated supercell with SG $X2/b$ ($t_0 = 0$) transformed (Fig. 5) by the matrix (2/5 −1/5 0; 1/5 2/5 0; 001) reproduces the experimental data. Both experimental and generated structures are described in the monoclinic SG $I2/b$ (Table 9). The *ab* structure projections are shown in Fig. 7. It should be noted that, according to Huyghe *et al.* (1991*b*), $K_4Th(MoO_4)_4$ and also probably $Li_4Np(MoO_4)_4$, $Li_4Pu(MoO_4)_4$, $Na_4Th(MoO_4)_4$, $Na_4Th(WO_4)_4$ and $Na_4Pu(MoO_4)_4$ are isotypic with $Na_4Zr[MoO_4]_4$.

3.3.5. Structure with ordering of cations on both *A* and *X* positions. The tetragonal structure of $Na_5Y(MoO_4)_4 = Na_4Y[Na'(MoO_4)_4]$ (Stedman *et al.*, 1994; Table 1) represents an interesting scheelite-like structure characterized by an ordered replacement of part of the anionic $[XO_4]$ groups by cations. The general formula can be written as $A'_4A''[A'''(X''O_4)_4]$. This structure is analogous to $A'_4A''[\diamond(X''O_4)_4] = Na_4Zr[(MoO_4)_4]$, as described above. One-fifth of the $[XO_4]$ positions is vacant in $Na_4Zr[(MoO_4)_4]$, while these vacancies are occupied by extra Na ions in $Na_4Y[Na'(MoO_4)_4]$. Hence, its generation can proceed along the same line. This is illustrated in Fig. 7. A comparison of the generated atomic coordinates with the experimental data is shown in Table 10. The structure is found in $Na_5Tb(MoO_4)_4$, $Na_5Tb(MoO_4)_4$, $Na_5Lu(MoO_4)_4$, $Na_5Lu(WO_4)_4$ (Efremov *et al.*, 1980) and some other phases $A_5M(XO_4)_4$ (A = Li, Na; M = La to Lu, Y; X = Mo or W; Stedman *et al.*, 1994).

3.4. Incommensurate modulated $KNd[MoO_4]_2$ structure as a starting model for refinement

Besides being used for the derivation of the three-dimensional structures, the incommensurately modulated structure $KNd[MoO_4]_2$ has also been used as a starting model for the refinement of another incommensurately modulated scheelite-like structure, $KSm[MoO_4]_2$ (Arakcheeva *et al.*, 2007). This structure differs mainly by the A position occupation function (Table 1, Figs. 2 and 3), which is a variable in the proposed superspace model (see §3.2). The refined fractional atomic coordinates in the common basic unit cell are identical within 2σ and 8σ, respectively (Table 11). Therefore, these two incommensurately modulated structures, which differ in their composition and occupation functions, still share an identical basic structure within the unique SSG.

It is worth mentioning that, for the structures we considered, the atomic coordinates of the three-dimensional structures projected in the basic unit cell (SG *I*2/*b*) and averaged are very similar to each other and also to the basic structure of two (3 + 1)-dimensional compounds (Table 11). This justifies the use of a single superspace model as provided by the incommensurate $KNd[MoO_4]_2$ to derive the three-dimensional members of the family.

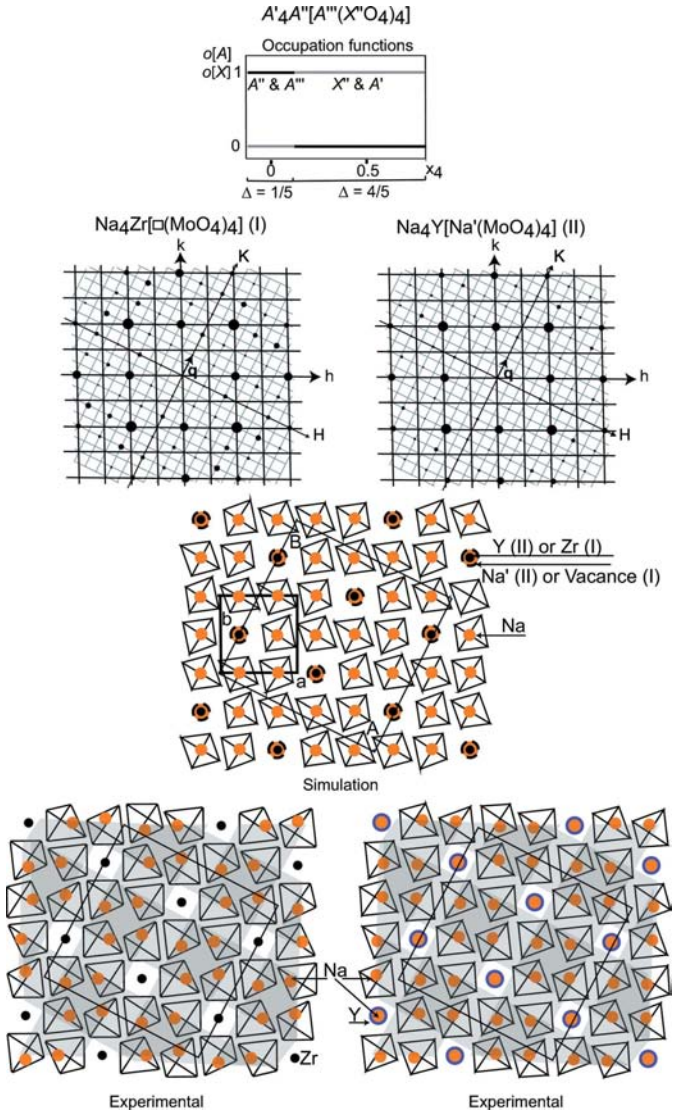

Figure 7
Representation of the $Na_4Zr[(MoO_4)_4]$ and $Na_4Y[Na'(MoO_4)_4]$ tetragonal scheelite-like structures generated from the incommensurately modulated structure of $KNd(MoO_4)_2$. The crenel occupation functions (top) are established according to their general composition. The modulation vector **q** = 2/5**a*** + 4/5**b*** has been selected from the reciprocal space analysis (sections *hk*0 are presented). The *ab* projection of the common monoclinic model (simulation) is compared with the respective projection of the published tetragonal structures (experimental). The experimental (thin lines) and basic (bold lines) unit cells are indicated in the *ab* projections. The $[MoO_4]$ groups are indicated by tetrahedra. The grey and white areas show two orthogonal systems of compositional waves. Notations in the *hk*0 sections are similar to those in Fig. 3.

3.5. The predictive capability of the incommensurately modulated structure $KNd[MoO_4]_2$

As mentioned above, compounds with sheelite-like structures are currently investigated owing to their application for

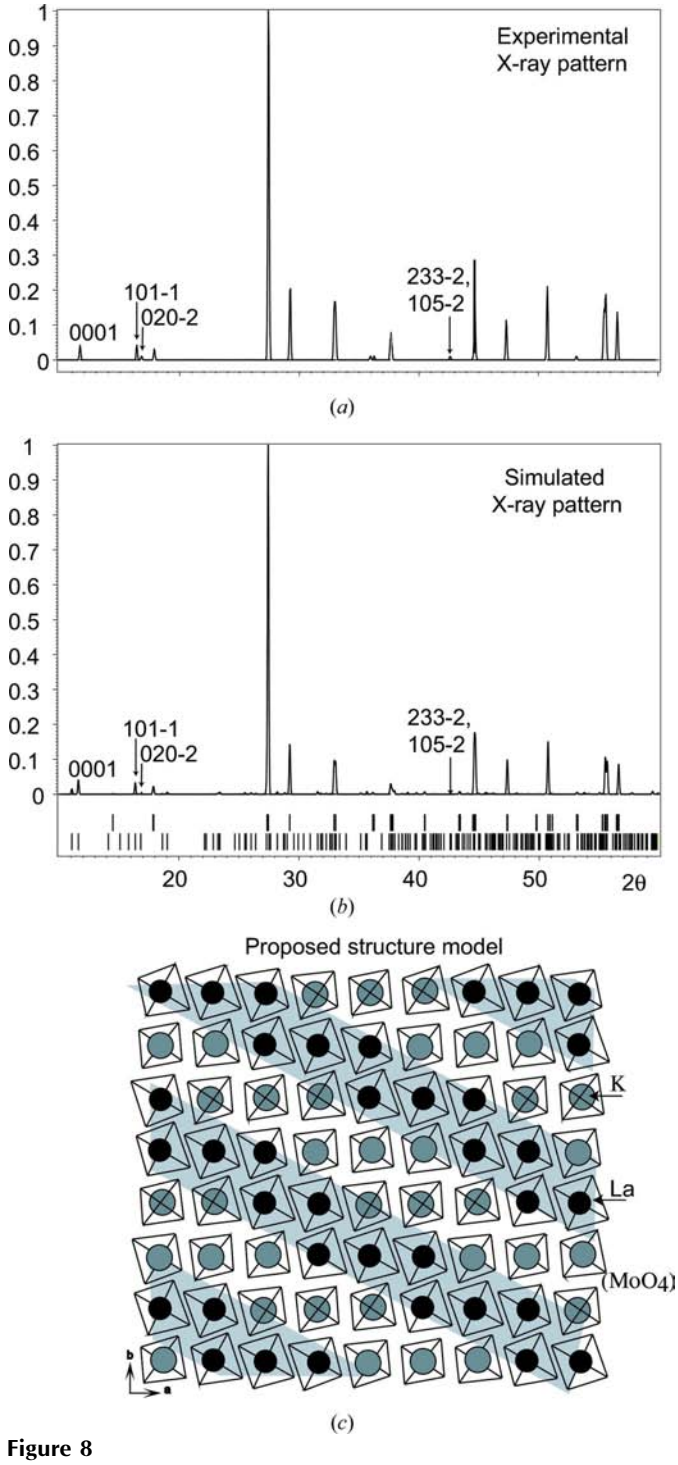

Figure 8
Prediction of the $KLa[MoO_4]_2$ crystal structure. Experimental and simulated X-ray patterns correspond to Cu $K\alpha$ radiation. Positions of main (upper level) and satellite (lower level) reflections are shown at the bottom of the simulated X-ray pattern. The four-component *hklm* indices are indicated only for previously non-indexed reflections. The proposed incommensurately modulated structure model is illustrated in the *ab* projection.

Table 11
Comparison of the basic structure atomic coordinates refined for the incommensurately modulated structures $KNd(MoO_4)_2$ and $KSm(MoO_4)_2$, and average atomic coordinates calculated for three-dimensional scheelite-like structures in the monoclinic basic unit cell (SG $I2/b$; $a/b \simeq 1$, $c/a \simeq c/b \simeq 2$, $a \simeq 5.5$ Å, $\gamma \simeq 90°$; A [4(e) $\frac{1}{2}$ 1/4 z], X [4(e): $\frac{1}{2}$ 1/4 z], O1 [8(f): xyz], O2 [8(f): xyz].

Parameter	KNd-$(MoO_4)_2$	KSm-$(MoO_4)_2$	RbBi-$(MoO_4)_2$	K_2Th-$(MoO_4)_3$	$Bi_3(FeO_4)$-$(MoO_4)_2$	Bi_2-$(MoO_4)_3$	La_2-$(MoO_4)_3$	Na_4Zr-$(MoO_4)_4$	Na_5Y-$(MoO_4)_4$	$CaWO_4$
A: $z_{A'}$	0.889 (1)	0.885 (3)	0.8763	0.8631	0.8868	0.8612	0.8754	0.875	0.875	0.875
$z_{A''}$	0.880 (2)	0.875 (3)								
X: z	0.3774 (2)	0.3778 (2)	0.371	0.3745	0.3822	0.3878	0.3713	0.375	0.375	0.375
O1: x	0.3600 (1)	0.3566 (6)	0.3575	0.380	0.347	0.3701	0.3668	0.340	0.347	0.3493
y	0.0203 (12)	0.0107 (8)	0.023	0.013	0.018	−0.093	0.0122	0.0013	0.011	−0.0086
z	0.2928 (5)	0.2920 (3)	0.284	0.299	0.2985	0.196	0.3023	0.291	0.287	0.2894
O2: x	0.7744 (13)	0.7635 (8)	0.7885	0.769	0.749	0.7625	0.7843	0.751	0.761	0.7414
y	0.3936 (10)	0.4043 (7)	0.393	0.407	0.427	0.3942	0.4078	0.410	0.403	0.4007
z	0.0429 (5)	0.0428 (3)	0.046	0.060	0.0394	0.0503	0.0509	0.041	0.037	0.0394

solid-state lasers. However, their crystal structures are usually characterized on the basis of strong reflections only. A row of compounds with the general composition $A'A''[X'O_4]_2$ [tetragonal $AgTb(MoO_4)_2$ reported by Shi *et al.* (1996*b*); $LiYb(MoO_4)_2$ in Volkov *et al.* (2005); $NaLa(MoO_4)_2$ and $NaCe(MoO_4)_2$ in Teller (1992), and some others] have been described in the simplest tetragonal scheelite structure type with cations randomly distributed on the A site. Weak extra reflections occurring in the lower-angle range of the X-ray pattern have been ignored, probably because they cannot be indexed in any three-dimensional unit cell; sometimes, the lower-angle part of the diffraction pattern is not represented. As was shown with the examples $KNd[MoO_4]_2$ (Morozov *et al.*, 2006) and $KSm[MoO_4]_2$ (Arakcheeva *et al.*, 2007), the modulated scheelite-like structures exhibit typical series of lower-angle reflections. Therefore, the compounds mentioned are good candidates for structure reinvestigations in the superspace group $I2/b(\alpha\beta0)00$ based on the $KNd[MoO_4]_2$ model. Two examples are presented here.

For the scheelite-like phase of $KEu(MoO_4)_2$ (PDF2 No. 31-1006 in the JCPDS database) the indexing of the series of lower-angle reflections is missing, because they cannot be indexed in the selected unit cell. Using $KNd[MoO_4]_2$ as a (3 + 1)-dimensional superspace model (replacing Nd by Eu) and the experimental powder diffraction pattern from the database, we refined the basic unit-cell parameters, the modulation vector **q** (Table 1), indexed the whole set of experimental reflections and calculated their intensities (Morozov *et al.*, 2006). The high accuracy of the refined lattice constants and the good agreement between the calculated and experimental intensities (Table 6 in Morozov *et al.*, 2006) indicate that $KEu(MoO_4)_2$ has an incommensurately modulated structure, which is similar to $KNd[MoO_4]_2$.

The space group and standard deviations of the unit-cell parameters of another scheelite-like compound, $KLa[MoO_4]_2$ (Potapova *et al.*, 1987), are missing in the ICDD database (PDF-00-040-0466). This is probably due to some unindexed reflections. We refined the given unit-cell parameters (a = 5.417, b = 5.437, c = 12.205 Å, γ = 90.05°) along with a modulation vector **q** in the SSG $I2/b(\alpha\beta0)00$. The resulting values [a = 5.41732 (12), b = 5.43739 (12), c = 12.2121 (2) Å, γ = 90.052 (2)° and $\mathbf{q} = 0.35069\ (5)\mathbf{a}^* + 0.62216\ (4)\mathbf{b}^*$] allow us to index all 89 reflections, including the neglected ones (Fig. 8 top). These lattice constants and the $KNd[MoO_4]_2$ structure model (with replacement Nb by La) have been used for the simulation of the X-ray powder diffraction pattern (Fig. 8*b*). Unfortunately, the quality of the experimental data taken from the database does not allow us to complete the structure refinement. Intensities are given relative to the strongest (I = 100%) reflection, which is probably underestimated (Fig. 8). Nevertheless, the comparison of all other experimental and simulated reflections indicates that $KLa[MoO_4]_2$ also belongs to the incommensurately modulated scheelite-like structures (Fig. 8*c*).

3.6. Capabilities and limitations of the incommensurately modulated $KNd[MoO_4]_2$ structure as a natural superspace model

We have seen that it is possible to derive known three-dimensional and (3 + 1)-dimensional structures and index some problematic X-ray patterns using $KNd[MoO_4]_2$. Thus, the incommensurately modulated structure of $KNd[MoO_4]_2$ can be exploited as a natural superspace model for the characterization of the (3 + 1)-dimensional scheelite-like family described in §3.2.

The results of the three-dimensional scheelite-like structure derivations (Tables 3–10, Figs. 6 and 7) show that these three-dimensional structures along with the (3 + 1)-dimensional incommensurately modulated structures $KNd[MoO_4]_2$ and $KSm[MoO_4]_2$ can be characterized as one family sharing a common superspace group, a common number of building units in the common basic unit cell occupying the same Wyckoff sites (Table 1). Despite a wide variation of chemical composition observed in the family, the topology of each member (distribution of building units on A and X positions) can be completely predicted from $KNd[MoO_4]_2$ using the appropriate modulation vector **q**, occupation functions and t_0 (listed in Table 1 for each known compound). The space-group symmetry, the unit cell and Wyckoff sites can also be completely reproduced for each three-dimensional monoclinic structure. These deductive capabilities of the incommensu-

rately modulated structure, for the structures we considered, can be exploited for the generation and prediction of other members of the scheelite-like family. The vector **q** can be widely varied for each possible type of occupation function applied for both the *A* and *X* position.

3.6.1. Symmetry limitations. When special relations occur between rational α and β components of the modulation vector **q** (including $\alpha = \beta = 0$ for $CaWO_4$), the derived monoclinic three-dimensional structure can also exhibit pseudo-tetragonal symmetry {with SG *I*2/*b* for $Na_4Zr[MoO_4]_4$, $Na_4Y[Na'(MoO_4)_4]$ and $CaWO_4$}, and tetragonal supergroups as experimentally determined {$I4_1/a$ for $Na_4Zr[MoO_4]_4$, $Na_4Y[Na'(MoO_4)_4]$ and $CaWO_4$}. On one hand, this limits the capacity of the superspace model for degenerate structures. On the other hand, the lower symmetry derived from the SSG points to the probability of lower symmetry under some specific conditions. Indeed, the high-pressure modification of $CaMoO_4$ (Crichton & Grzechnik, 2004) exhibits exactly the proposed monoclinic symmetry (SG *I*2/*b*, $a = 5.108$, $b = 5.034$, $c = 10.768$ Å, $\gamma = 90.96^\circ$), while the room-temperature modification is isotypic with tetragonal scheelite, $CaWO_4$. The lower-temperature phase transition associated with a monoclinic distortion of the tetragonal scheelite structure type is very frequently observed, for example in $NaBi(MoO_4)_2$ (Waskowska *et al.*, 2005), $BiVO_4$, $LaNbO_4$, $CaMoO_4$ and many rare-earth niobates, tantalates among others (Jeitschko *et al.*, 1976).

3.6.2. Topological limitations. In this work we only considered the main manifold of the scheelite-like structures, where an ordering occurs in the *ab* plane, whereas the $c \simeq 2a_{basic}$ translation remains unchanged. A few known structures, with ordering on the *A* and *X* position along the *c* axis with $a \simeq b \simeq a_{basic}$, are beyond the scope of the family described with $\mathbf{q} = \alpha\mathbf{a}^* + \beta\mathbf{b}^*$. For example, the scheelite-like structure of the mineral paraniite, $(CaWO_4)_2(YAsO_4)$, SG $I4_1/a$, $a = 5.135$ (1), $c = 33.882$ (5) Å (Demartin *et al.*, 1994), cannot belong to this family owing to the triple parameter $c \simeq 6a_{basic}$ pointing to a commensurate modulation along the *c* axis.

3.6.3. Accuracy of variables derived from the incommensurately modulated $KNd[MoO_4]_2$ structure. Taking into account the wide selection of elemental and chemical compositions in the scheelite-like structure representatives, one can say that the fractional coordinates of the building units (*A* and *X* positions) derived from the $KNd[MoO_4]_2$ structure are in good agreement with the experimental values (Tables 3–10). For example, the difference between two structure determinations performed for $K_2Th[MoO_4]_2$ is comparable with the difference between them and the derived structure (Table 4). Deviations (δ) of the derived fractional coordinates from the experimental ones vary from 0 to 0.07 depending on the elemental composition and presence or absence of vacancies (Tables 3–10). The best result is for $K_2Th[MoO_4]_2$ ($\delta < 0.005$ for five and $\delta < 0.03$ for two variables, Table 3). The worst result is observed for $Bi_2(MoO_4)_3$ (Table 6), where 1/3 of *A* positions are vacant rather than K. The crystal chemistry of Bi is also quite different from Nb. The reproducibility is much better when Bi is replaced by La in $La_2(MoO_4)_3$ (Table 5) or by Eu in $Eu_2(MoO_4)_3$ (Table 7).

The main difference between derived and experimental structures is observed for the oxygen positions (Figs. 6 and 7). All O atoms occupy the general sites in the corresponding SGs. Deviations of their positions from the model indicate mainly tilts of the $[XO_4]$ tetrahedra; these tilts define the specificity of each compound (Figs. 6 and 7). In spite of the essential difference between experimental and derived fractional coordinates of the O atoms, the shifts and tilts observed for $[XO_4]$ tetrahedra in the experimental structures are clearly visible as tendencies in the derived structures (Figs. 6 and 7). Again, the most and the least reproducible structure is $K_2Th[MoO_4]_2$ and $Bi_2(MoO_4)_3$, respectively, because shifts and tilts of $[XO_4]$ tetrahedra are governed by the interatomic distances, which are as far from the model as the chemical composition of a derived compound is far from the chemical composition of the model.

3.7. Physical significance of the modulation vector q in the scheelite-like family

The (3 + 1)-dimensional presentation of the scheelite-like family with a unique superspace model based on the incommensurately modulated $KNd[MoO_4]_2$ structure does reveal the common origin of the structure modulation as a composition-ordering wave running in the *ab* plane (Figs. 3, 4, 7 and 8). This wave is uniquely defined by the modulation vector **q**. The length of this wave can be either commensurate or incommensurate relative to the *a* and *b* parameters of the basic structure. The distribution of the composition along the modulation wave is just the occupation function. The intersection of the compositional wave with the *A* and *X* atomic positions defines the composition of these positions. In the (pseudo)-tetragonal structures (Fig. 6), the superposition of two orthogonal waves creates columns of Zr vacancies and Y—Na′ extending along the *c* axis.

As can be deduced from Table 1, Figs. 3, 4 and 7, the true direction of the compositional wave is not immediately clear either from the general composition (three different **q** vectors do exist for $A'A''[X'O_4]_2$) or from the chemical composition. For example, $K_2Th[MoO_4]_3$ and $Bi_3[FeO_4][MoO_4]_2$ are characterized by the same modulation vector **q**.

One should emphasize that the compositional wave is difficult to recognize from the traditional three-dimensional presentation of the crystal structures (Fig. 6), especially if they are considered separately.

4. Discussion

With the example of the scheelite-like family of structures, we propose one novel application of an incommensurately modulated structure. We propose to exploit an incommensurately modulated structure as a natural superspace model to describe and also predict a family of both incommensurately and commensurately modulated structures characterized by a

wide range of elemental and chemical composition and topology.

The proposed application of an incommensurately modulated structure as a natural superspace model can be considered as a top-down approach of the superspace concept in comparison to the widely developed bottom-up approach (Evain *et al.*, 1998; Gourdon *et al.*, 2000; Boullay *et al.*, 2002; Elcoro *et al.*, 2000, 2001, 2003, 2004; Schönleber *et al.*, 2004; Lind & Lidin, 2003; Chen & Walker, 1990, among others). In the bottom-up approach, the superspace model is constructed by inference in order to fit the topological and symmetrical characteristics of the series of known related structures. In the proposed top-down approach, a superspace model is taken as a refined incommensurately modulated structure. For such a model, the SSG and the basic structure have already been determined and refined on the basis of experimental data. The most obvious modulations observed in the structure (displacive or occupation modulations) point to the primary variables. In both top-down and bottom-up approaches, the topological manifold of the structures can be derived or generated from the superspace model by variations in the modulation vector **q**, and occupation functions and/or atomic displacive modulations, while SGs of three-dimensional members depend in addition on t_0.

Estimation of limitations of the $KNd(MoO_4)_2$ incommensurately modulated structure as the superspace model for the generation of the (3 + 1)-dimensional scheelite family reveals the following features, which can be regarded as general limitations when an incommensurately modulated structure is used as a superspace model. First, the SG symmetry of a generated three-dimensional structure cannot be higher than the SSG symmetry of the model, even if the topology of the generated structure can be considered as a pseudo-higher symmetric one. In this case, the possibility of a supergroup has to be considered for such a degenerate three-dimensional structure. The second limitation concerns the topological manifold of a generated family. This manifold is restricted to the SSG. The next limitation concerns the variability of atomic coordinates, which are not fixed by the SG of three-dimensional structures and which are variable in incommensurately modulated structures. These coordinates, respectively atomic displacive modulations, can be derived from the model with accuracy, which is dependent on the chemical composition of both the generated structure and the incommensurately modulated structure taken as a superspace model. The closer their chemical composition, the more precise are the derived coordinates.

An incommensurately modulated structure considered as a natural superspace model allows a clear identification of the constants and variables in the corresponding $(3 + d)$-dimensional family. Moreover, the constants, consisting of the SSG, a number of building units occupying certain Wyckoff sites and basic lattice parameters (ratios a/b, b/c, c/a and angles), represent attributes of each $(3 + d)$-dimensional family containing both commensurate and incommensurate structures independently of their elemental composition. One can compare these characteristics with the definition of the structure type (Parthé, 1996; Lima-de-Faria *et al.*, 1990; Allmann & Hinek, 2007). The comparison indicates that the definition of a (three-dimensional) structure type differs from the listed characteristics of the $(3 + d)$-dimensional family, which can be derived from an incommensurately modulated structure, by replacing the SG by the SSG. This means that an incommensurately modulated structure can also be used for the characterization of a $(3 + d)$-dimensional structure type. In the present work, the description of the scheelite-like family is indeed a description of the (3 + 1)-dimensional scheelite structure type.

The example of the (3 + 1)-dimensional scheelite structure type family shows (Arakcheeva & Chapuis, 2006*b*):

(i) the term 'structure type' can be generalized in higher-dimensional space by replacing the common SG request by the common SSG request in its definition;

(ii) many related three-dimensional structures differing by SG and unit-cell geometry (ratios a/b, b/c, c/a and angles) can be combined in a single $(3 + d)$-dimensional structure type along with $(3 + d)$-dimensional structures, while such a combination is not possible in the frame of a single three-dimensional structure type.

It should be emphasized that a $(3 + d)$-dimensional structure can only be embedded in a $(3 + d)$-dimensional structure-type family because such a structure is obviously outside any three-dimensional structure type family. For example, the commensurately and incommensurately modulated structures observed in the $NiGe_{1-x}P_x$ solid solution [$Amam(00\gamma)s00$ SSG; basic structure of NiAs-type; γ coefficient of the **q** vector is compositionally dependent] have been characterized by Larsson *et al.* (2007) as a 'continuously variable, incommensurately modulated, intermediate structure type providing a natural link or bridge between the two extreme end-member structures, *i.e.* NiGe (of MnP structure type) and NiP by simply choosing the commensurate option with $\gamma = 1$ and $\frac{1}{2}$, respectively'. Assuming these results and the generalization of the structure type term in $(3 + d)$-dimensional space proposed here, both the modulated $NiGe_{1-x}P_x$ structures and the end-members can be considered as the single (3 + 1)-dimensional NiAs structure type, which is not 'continuously variable and incommensurately modulated'. It would be interesting to consider other NiAs-related compounds as members of this (3 + 1)-dimensional NiAs structure type.

5. Summary

With the example of the scheelite-like incommensurately modulated structure (3 + 1)-dimensional $KNd[MoO_4]_2$ applied here for the description and derivation of scheelite-like compounds differing widely in chemical composition and topology, we have shown that an incommensurately modulated structure can be used as a natural superspace model, capable of generating and describing a family of compounds belonging to a unique higher-dimensional structure type. This superspace model and the corresponding higher-dimensional structure type are characterized by the SSG, a number of building units in some basic unit-cell occupying certain

Wyckoff sites. In this model and in the corresponding structure type, the occupation and displacive atomic modulations along with the free coefficients of the vector **q** are variables. An incommensurately modulated structure taken as a superspace model indicates the primary variable(s), which is (are) responsible for the structure manifold in the structure-type family. Other parameters of a generated structure can be predicted from this model with accuracy, depending on the chemical composition: the closer the composition of the generated structure is to the composition of the model, the higher the accuracy of the derived variables that can be achieved. The symmetry of the three-dimensional structures and topological manifold in the structure type family are restricted by the SSG.

We would like to thank Ivan Orlov for his helpful discussion on the possible space groups derived from $I2/b(\alpha\beta0)00$. This work has been performed with the support of the Swiss National Science foundation (grant Nos. 20-105325/1 and 200021-109470/1), which is gratefully acknowledged.

References

Allmann, R. & Hinek, R. (2007). *Acta Cryst.* A**63**, 412–417.
Arakcheeva, A. & Chapuis, G. (2006*a*). *Acta Cryst.* B**62**, 52–59.
Arakcheeva, A. & Chapuis, G. (2006*b*). *Acta Cryst.* A**62**, s46.
Arakcheeva, A., Filaretov, A., Pattison, P., Chapuis, G., Rossell, M., Morozov, V. & Van Tendeloo, G. (2008). *Acta Cryst.* Submitted for publication.
Boullay, Ph., Trolliard, G., Mercurio, D., Perez-Mato, J. M. & Elcoro, L. (2002). *J. Solid State Chem.* **164**, 252–260.
Bushuev, N. N. & Trunov, V. K. (1976). *Kristallografiya*, **21**, 69–72.
Chen, Z. Y. & Walker, M. B. (1990). *Phys. Rev. B*, **43**, 5634–5648.
Crichton, W. A. & Grzechnik, A. (2004). *Z. Kristallogr. New Cryst. Struct.* **219**, 337–338.
Demartin, F., Gramaccioli, C. M. & Pilati, T. (1994). *Schweiz. Miner. Petro. Mitt.* **74**, 55–60.
Efremov, V. A., Berezina, T. A., Averina, I. M. & Trunov, V. K. (1980). *Kristallografiya*, **25**, 254–261.
Elcoro, L., Perez-Mato, J. M., Darriet, J. & El Abed, A. (2003). *Acta Cryst.* B**59**, 217–233.
Elcoro, L., Perez-Mato, J. M. & Withers, R. (2000). *Z. Kristallogr.* **215**, 727–739.
Elcoro, L., Perez-Mato, J. M. & Withers, R. L. (2001). *Acta Cryst.* B**57**, 471–484.
Elcoro, L., Zúñiga, F. J. & Perez-Mato, J. M. (2004). *Acta Cryst.* B**60**, 21–31.
Elzen, A. F. van den & Rieck, G. D. (1973). *Acta Cryst.* B**29**, 2433–2436.
Evain, M., Boucher, F., Gourdon, O., Petříček, V., Dušek, M. & Bezdicka, P. (1998). *Chem. Mater.* **10**, 3068–3076.
Gourdon, O., Petricek, V. & Evain, M. (2000). *Acta Cryst.* B**56**, 409–418.
Hazen, R. M., Finger, L. W. & Mariathasan, J. W. E. (1985). *J. Phys. Chem. Solids*, **46**, 253.
Huyghe, M., Lee, M.-R., Quarton, M. & Robert, F. (1991*a*). *Acta Cryst.* C**47**, 244–246.
Huyghe, M., Lee, M. R., Quarton, M. & Robert, F. (1991*b*). *Acta Cryst.* C**47**, 1797–1799.
Janssen, T., Chapuis, G. & de Boissieu, M. (2007). *Aperiodic Crystals. From Modulated Phases to Quasicrystals.* Oxford University Press.
Jeitschko, W. (1973). *Acta Cryst.* B**29**, 2074–2081.
Jeitschko, W., Sleight, A. W., McClellan, W. R. & Weiher, J. F. (1976). *Acta Cryst.* B**32**, 1163–1170.
Klevtsova, R. F., Gaponenko, L. A., Glinskaya, L. A., Zolotova, E. S., Podberezskaya, N. V. & Klevtsov, P. V. (1979). *Kristallografiya*, **24**, 751–756.
Klevtsova, R. F., Solov'eva, L. P. & Vinokurov, V. A. (1975). *Kristallografiya*, **20**, 270–275.
Kolitsch, U. & Tillmanns, E. (2003). *Acta Cryst.* E**59**, i43–i46.
Larsson, A.-K., Garcia-Garcia, F. J. & Withers, R. L. (2007). *J. Solid State Chem.* **180**, 1093–1102.
Lee, A. van der & Evain, M. (1995). *Aperiodic'94*, edited by G. Chapuis and V. Petříček, pp. 440–444. Singapore: World Scientific Publishing.
Lima-de-Faria, J., Hellner, E., Liebau, F., Makovicky, E. & Parthé, E. (1990). *Acta Cryst.* A**46**, 1–11.
Lind, H. & Lidin, S. (2003). *Solid State Sci.* **5**, 47–57.
Morozov, V. A., Arakcheeva, A. V., Chapuis, G., Gublin, N., Rossell, M. D. & Van Tendeloo, G. (2006). *Chem. Mater.* **18**, 4075–4082.
Neeraj, S., Kijima, N. & Cheetham, A. K. (2004). *Chem. Phys. Lett.* **387**, 2–6.
Orlov, I., Palatinus, L., Arakcheeva, A. & Chapuis, G. (2007). *Acta Cryst.* B**63**, 703–712.
Orlov, I., Schoeni, N. & Chapuis, G. (2007). Superspace Finder – Web database of three-dimensional derivatives for (3+1)D space groups in analytical form. Ecole Polytechnique Fédérale de Lausanne, Lausanne, Switzerland, http://superspace.epfl.ch/finder/.
Palatinus, L., Dušek, M., Glaum, R. & El Bali, B. (2006). *Acta Cryst.* B**62**, 556–566.
Parthé, E. (1996). *Elements of Inorganic Structural Chemistry.* Petit-Lancy, Switzerland: Sutter K Parthé Publisher. I-1.
Pearson, W. B. (1972). *The Crystal Chemistry and Physics of Metals and Alloys*, pp. 15–19. New York: Wiley-Interscience.
Perez-Mato, J. M., Madariaga, G., Zuñiga, F. J. & Garcia Arribas, A. (1987). *Acta Cryst.* A**43**, 216–226.
Perez-Mato, J. M., Zakhour-Nakhl, M., Weill, F. & Darriet, J. (1999). *J. Mater. Chem.* **9**, 2795–2808.
Petříček, V., Dušek, M. & Palatinus, L. (2000). *JANA*2000. Institute of Physics, Praha, Czech Republic.
Potapova, O., Protasova, V. & Kharchenko, L. (1987). *Russ. J. Inorg. Chem.* **32**, 1703.
Schönleber, A., Zúniga, F. J., Perez-Mato, J. M., Breczewski, T. & Darriet, J. (2004). *Acta Cryst.* A**60**, s186.
Shi, F., Meng, J. & Ren, Y. (1996*a*). *J. Solid State Chem.* **121**, 236–239.
Shi, F., Meng, J. & Ren, Y. (1996*b*). *J. Alloys Compd.* **233**, 56–60.
Shi, F., Meng, J., Ren, Y. & Su, Q. (1997). *J. Phys. Chem. Solids*, **59**, 105–110.
Sleight, A. W., Chen, H.-Y., Ferretti, A. & Cox, D. E. (1979). *Mater. Res. Bull.* **14**, 1571–1581.
Smaalen, S. van (2004). *Z. Kristallogr.* **219**, 681–691.
Stedman, N. J., Cheetham, A. K. & Battle, P. D. (1994). *J. Mater. Chem.* **4**, 707–711.
Teller, R. G. (1992). *Acta Cryst.* C**48**, 2101–2104.
Templeton, D. H. & Zalkin, A. (1963). *Acta Cryst.* **16**, 762–766.
Theobald, F. R. & Laarif, A. (1985). *Mater. Res. Bull.* **20**, 653–665.
Volkov, V., Cascales, C., Kling, A. & Zaldo, C. (2005). *Chem. Mater.* **17**, 291–300.
Waskowska, A., Gerward, L., Staun Olsen, J., Maczka, M., Lis, T., Pietraszko, A. & Morgenroth, W. (2005). *J. Solid State Chem.* **178**, 2218–2224.
Wolff, P. M. de, Janssen, T. & Janner, A. (1981). *Acta Cryst.* A**37**, 625–636.
Yamamoto, A. & Nakazawa, H. (1982). *Acta Cryst.* A**38**, 79–86.